Structural Engineering and Mechanics, *Vol. 59, No. 3 (2016) 579-599*
DOI: http://dx.doi.org/10.12989/sem.2016.59.3.579

Analytical solutions for static bending of edge cracked micro beams

Şeref Doğuşcan Akbaş*

Department of Civil Engineering, Bursa Technical University, Bursa, Turkey

(Received August 24, 2015, Revised May 25, 2016, Accepted June 10, 2016)

Abstract. In this study, static bending of edge cracked micro beams is studied analytically under uniformly distributed transverse loading based on modified couple stress theory. The cracked beam is modelled using a proper modification of the classical cracked-beam theory consisting of two sub-beams connected through a massless elastic rotational spring. The deflection curve expressions of the edge cracked microbeam segments separated by the rotational spring are determined by the Integration method. The elastic curve functions of the edge cracked micro beams are obtained in explicit form for cantilever and simply supported beams. In order to establish the accuracy of the present formulation and results, the deflections are obtained, and compared with the published results available in the literature. Good agreement is observed. In the numerical study, the elastic deflections of the edge cracked micro beams are calculated and discussed for different crack positions, different lengths of the beam, different length scale parameter, different crack depths, and some typical boundary conditions. Also, the difference between the classical beam theory and modified couple stress theory is investigated for static bending of edge cracked microbeams. It is believed that the tabulated results will be a reference with which other researchers can compare their results.

Keywords: open edge crack; modified couple stress theory; cracked microbeam

1. Introduction

With the great advances in technology in recent years, micro and nano structures have found many applications. In these structures, micro beams and micro tubes are widely used in micro- and nano electromechanical systems (MEMS and NEMS) such as sensors (Zook *et al*. 1992, Pei *et al*. 2004), actuators (Senturia 1998, Rezazadeh *et al*. 2006), biosensors, atomic-force microscopes, vibration sensors, micro-probes. In investigation of micro and nano structures, the classical continuum mechanics which is scale independent theories, are not capable of explanation of the size-dependent behaviors. Nonclassical continuum theories such as higher order gradient theories and the couple stress theory are capable of explanation of the size dependent behaviors which occur in micro-scale structures.

At the present time, the experimental investigations of the micro/nano materials are still a challenge because of difficulties confronted in the micro/nano scale. Hence, mathematical model

*Corresponding author, Associate Professor, E-mail: serefda@yahoo.com

http://www.techno-press.org/?journal=sem&subpage=8 ISSN: 1225-4568 (Print), 1598-6217 (Online)

and atomistic simulations have been used for micro structural analysis. The process of the atomistic simulations are very difficult and take much time. So, the researchers have attempted to simplified models for mechanical analyzing of the micro/nano structures. In the mechanical modelling of the micro/nano structures, micro and nano systems are modelled structural elements such as plate, shell and beams. Also, Continuum theory is the most preferred method for the analysis of the micro and nano structures in the mechanical modelling. Size effects are very important parameter in the structural behavior of micro/nano structures, because the dimensions of these structures are smaller than the atomic/molecular distances. Classical continuum mechanics does not contain the size effect, because of its scale-free character. To take account of the size effect, The nonlocal continuum theory initiated by Eringen (1972) which has been widely used to mechanical behavior of nano-micro structures.

Micro and nano structures are subjected to destructive effects in the form of initial defects within the material or caused by fatigue or stress concentration, for example, crack occurrence in ZnO nano-rods is due to thermal fabrication process (Fang *et al*. 2003a, b). As a result of destructive effects, cracks occur in the structural elements. It is known that cracks cause local flexibility and changes in structural stiffness. Understanding the mechanical behaviour edge-cracked micro structures and detection of cracks are very important for safety of micro structures.

The size effect plays an important role on the mechanical behavior of microstructures at the micrometer scale that the classic theory has failed to consider when the size reduces from macro to nano (Toupin 1962, Mindlin 1962, Mindlin 1963, Fleck and Hutchinson 1993, Yang *et al.* 2002, Lam *et al*. 2003). Therefore, higher-order theories modified couple stress theory and modified strain gradient are used in the mechanical model of the nano-micro structures (Yang *et al* 2002, Lam *et al*. 2003).

The determination of the micro-structural material length scale parameters is very difficult experimentally. So, Yang *et al*. (2002) proposed the modified couple stress theory (MCST) in which the strain energy has been shown to be a quadratic function of the strain tensor and the symmetric part of the curvature tensor, and only one length scale parameter is included. After this, the MCST and the strain gradient elasticity theories have been widely applied to static and dynamic analysis of structures (Park and Gao 2006, Ma *et al*. 2008, Kong *et al*. 2008, Asghari *et al*. 2010, Wang 2010, Şimşek 2010, Kahrobaiyan *et al*. 2010, Xia *et al*. 2010, Ke *et al*. 2011, Akgöz and Civalek 2012, Ansari *et al*. 2012, Şimşek *et al*. 2013, Wang *et al.* 2013, Kocatürk and Akbaş 2013, Kong 2013, Alashti and Abolghasemi 2013, Ghayesh *et al*. 2013, Daneshmehr *et al*. 2013, Akgöz and Civalek 2013).

More recently, Darijani and Mohammadabadi (2014) proposed a new deformation beam theory for static and dynamic analysis of microbeams which includes unknown functions takes into account shear deformation and satisfies both of shear and couple-free conditions on the upper and lower surfaces of the beam based on a MCST. Tang *et al*. (2014) analyzed a theoretical model for flexural vibrations of microbeams in flow with clamped-clamped ends based on MCST. Sedighi *et al*. (2014) investigated the dynamic pull-in instability of vibrating micro-beams undergoing large deflection under electrosatically actuation. Beni and Zeverdejani (2015) studied free vibration of microtubules within elastic shell model by using MCST. Faraokhi *et al*. (2015) studied the three-dimensional motion characteristics of perfect and imperfect Timoshenko microbeams under mechanical and thermal forces based on the MCST. Zeighampour and Beni (2014, 2015), Zeighampour *et al*. (2015) investigated the shell structures within MCST. Ansari *et al*. (2015) studied an exact solution of vibrations of postbuckled microscale beams based on the MCST. Shojaeian and Beni (2015) presented the electromechanical buckling of beam-type nanoelectromechanical systems by considering the nonlinear geometric effect and intermolecular forces (based on MCST. Dai *et al*. (2015) developed a new nonlinear theoretical model for cantilevered microbeams and to explore the nonlinear dynamics based on the MCST, taking into account of one single material length scale parameter. Farokhi and Ghayesh (2015) investigated the three-dimensional motion characteristics of perfect and imperfect Timoshenko microbeams under mechanical and thermal forces. Sedighi and Bozorgmehri (2016) investigated dynamic instability of free-standing size-dependent nanowires by considering the Casimir force and surface effects with MCST. Beni *et al*. (2016) studied the functionally graded cylindrical thin shell by using MCST. Ataei *et al*. (2016) investigated Pull-in instability and free vibration of cantilever and clamped-clamped beam-type nanoactuators composud of functionally graded under the influence of electrostatic and intermolecular forces by using the modified strain gradient theory. Shojaeian *et al*. (2016) studied electromechanical buckling of beam-type nanoelectromechanical systems by using the modified strain gradient theory.

In the literature, the studies of the cracked micro-nano structures are as follows; Loya *et al*. (2009) studied the flexural vibrations of cracked micro- and nanobeams with the rotational and linear spring model based on nonlocal elasticity. Hasheminejad *et al*. (2011) investigated the flexural vibrations of cracked micro- and nanobeams in the presence of surface effects with the rotational linear spring model. Torabi and Nafar Dastgerdi (2012) studied with the free transverse vibration of cracked nanobeams modeled based on Eringen's nonlocal elasticity theory and Timoshenko beam theory with a rotational spring. Liu (2013) investigated vibration behavior of a cracked Euler-Bernoulli micro-cantilever beam under coupling action of nonlinear electrostatic force and squeeze film damping effect. Beni *et al*. (2015) examined the transverse vibration of cracked nano-beam based on MCST with rotational spring model. Akbaş (2016) studied the free vibration of functionally graded cracked micro beams based on MCST.

It is seen from literature that cracked beams has not been broadly investigated. A better understanding of the mechanism of how the cracks change response of static of a micro beam is necessary, and is a prerequisite for further exploration and application of the cracked micro beams.

This paper examines static bending of edge cracked microbeams analytically based on the MCST. The microbeams are subjected to uniformly distributed transverse loading. The microbeam model consist of the material length scale parameter which take into account the size effect. The cracked beam is modelled using a proper modification of the classical cracked-beam theory consisting of two sub-beams connected through a massless elastic rotational spring. The deflection curve expressions of the edge cracked microbeam segments separated by the rotational spring are determined by the integration method. The elastic curve functions of the edge cracked micro beams are obtained in explicit form for cantilever and simply supported beams. Some of the present results are compared with the previously published results to establish the validity of the present formulation. In the numerical study, the elastic deflections of the edge cracked micro beams are calculated and discussed for different crack positions, different lengths of the beam, different length scale parameter, different crack depths, and some typical boundary conditions. Also, the difference between the classical beam theory (CBT) and MCST is investigated for static bending of edge cracked microbeams.

The main purpose of the this study is investigation of using the classical cracked-beam model for the micro beams and determine the geometrical ratios in order to classical cracked-beam model can be used in the problems of the MCST. It is believed that the tabulated results will be a reference with which other researchers can compare their results.

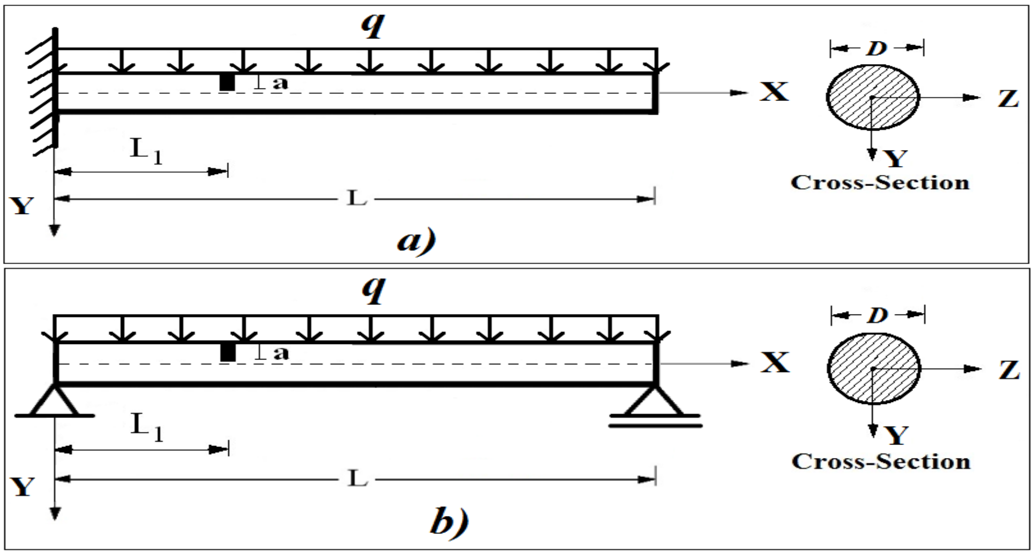

Fig. 1 Edge cracked circular micro beams with an open edge crack subjected to uniformly distributed transverse load (q) and cross-section. (a) Cantilever micro beam, (b) Simple supported micro beam

2. Theory and formulations

Fig. 1 shows cantilever and simple supported micro beams of length L, diameter D, containing an edge crack of depth a located at a distance from the left end L_1 with circular cross section. It is assumed that the crack is perpendicular to beam surface and always remains open. The beams are subjected to uniformly distributed transverse load (q) as seen from Fig. 1.

2.1 The modified couple stress theory

The strain energy density for a linear elastic material which is a function of both strain tensor and curvature tensor is introduced by Yang *et al*. (2002) for the MCST

$$U = \int_V (\sigma : \varepsilon + m : \chi)\, dV \tag{1}$$

where σ is the stress tensor, ε is the strain tensor, m is the deviatoric part of the couple stress tensor, χ is the symmetric curvature tensor, defined by

$$\sigma = \lambda\, tr(\varepsilon) I + 2\mu\varepsilon \tag{2}$$

$$\varepsilon = \frac{1}{2}[\nabla \boldsymbol{u} + (\nabla \boldsymbol{u})^T] \tag{3}$$

$$m = 2l^2 \mu\, \chi \tag{4}$$

$$\chi = \frac{1}{2}[\nabla \theta + (\nabla \theta)^T] \tag{5}$$

where λ and μ are Lame's constants, l is a material length scale parameter which is regarded as a material property characterizing the effect of couple stress, $\boldsymbol{u}$ is the displacement vector and θ is the rotation vector, given by

$$\theta = \frac{1}{2} \operatorname{curl} \boldsymbol{u} \tag{6}$$

The parameters λ and μ in the constitutive equation are given by

$$\lambda = \frac{E\,\nu}{(1+\nu)(1-2\nu)}\ , \quad \mu = \frac{E}{2(1+\nu)} \tag{7}$$

where E is the modulus of elasticity and ν is the Poisson ratio.

2.2 Governing equations of microbeams

According to the coordinate system (X,Y,Z) shown in Fig. 1, based on Euler-Bernoulli beam theory, the axial and the transverse displacement field are expressed as

$$u(X,Y) = -Y\frac{\partial v_0(X)}{\partial X} \tag{8}$$

$$v(X,Y,t) = v_0(X,t) \tag{9}$$

$$w(X,Y,t) = 0 \tag{10}$$

where u, v, w are x, y and z components of the displacements, respectively. Also, u_0 and v_0 are the axial and the transverse displacements in the mid-plane.

Because the transversal surfaces of the beam is free of stress, then

$$\sigma_{zz} = \sigma_{yy} = 0 \tag{11}$$

By using Eqs. (3), (8) and (9) and strain- displacement relation can be obtained

$$\varepsilon_{xx} = \frac{\partial u}{\partial X} = -Y\frac{\partial^2 v_0(X)}{\partial X^2} \tag{12a}$$

$$\varepsilon_{yy} = \varepsilon_{zz} = Y\frac{\nu(Y)\partial^2 v_0(X)}{\partial X^2} \tag{12b}$$

$$\varepsilon_{xz} = \varepsilon_{yz} = \varepsilon_{xy} = 0 \tag{12c}$$

By using Eqs. (6), (8), (9) and (10)

$$\theta_z = \frac{\partial v_0(X)}{\partial X}, \quad \theta_x = \theta_y = 0 \tag{13}$$

Substituting Eq. (13) into Eq. (5), the curvature tensor χ can be obtained as follows

$$\chi_{xz} = \frac{1}{2}\frac{\partial^2 v_0(X)}{\partial X^2},\ \chi_{xx} = \chi_{xy} = \chi_{yy} = \chi_{yz} = \chi_{zz} = 0 \tag{14}$$

According to Hooke's law, constitutive equations of the micro beam are as follows

$$\sigma_{xx} = E\,\varepsilon_{xx} = E\left[-Y\frac{\partial^2 v_0(X)}{\partial X^2}\right] \tag{15}$$

where σ_{xx} and ε_{xx} are normal stresses and normal strains in the X direction, respectively. Substituting Eq. (14) into Eq. (4), the couple stress tensor can be obtained as follows

$$m_{xz} = l^2\mu\frac{1}{2}\frac{\partial^2 v_0(X)}{\partial X^2} \tag{16a}$$

$$m_{xx} = m_{xy} = m_{yy} = m_{yz} = m_{zz} = 0 \tag{16b}$$

where μ is shear modulus which is defined by Eq. (7). Based on Euler-Bernoulli beam theory, the elastic strain energy (U_i) of the FG micro beam is expressed as

$$U_i = \frac{1}{2}\int_0^L \int_A \left(\sigma_{ij}\,\varepsilon_{ij} + m_{ij}\,\chi_{ij}\right) dA\, dX \tag{17}$$

By substituting Eqs. (15), (16), (12a) and (14) into Eq. (17), elastic strain energy (U_i) can be rewritten as follows

$$U_i = \frac{1}{2}\int_0^L \left[EA\left(\frac{\partial u_0}{\partial X}\right)^2 + EI\left(\frac{\partial^2 v_0}{\partial X^2}\right)^2 + \frac{1}{4}l^2\mu A\left(\frac{\partial^2 v_0}{\partial X^2}\right)^2\right] dX \tag{18}$$

where A is areas of the cross section, and I is the moment of inertia. The first variation of the strain energy is given as

$$\delta U = \int_0^L \left[EA\left(\frac{\partial u_0}{\partial X}\right)\left(\frac{\partial \delta u_0}{\partial X}\right) + EI\left(\frac{\partial^2 v_0}{\partial X^2}\right)\left(\frac{\partial^2 \delta v_0}{\partial X^2}\right) + \frac{1}{2}l^2\mu A\left(\frac{\partial^2 v_0}{\partial X^2}\right)\left(\frac{\partial^2 \delta v_0}{\partial X^2}\right)\right] dX \tag{19}$$

The potential energy of the external load can be written as

$$W = \int_{x=0}^{L} q(X)\, v_0(X)\, dx \tag{20}$$

The first variation of work done by the external applied forces is given as

$$\delta W = \int_{x=0}^{L} q(X)\, \delta v_0(X)\, dx \tag{21}$$

where q is uniformly distributed transverse load. Based on the minimum total potential energy principle, the first variation of the total potential energy is as follows

$$\delta\Pi = \delta(U - W) = 0 \tag{22}$$

where Π is the total potential energy. Substituting Eqs. (19) and (21) into Eq. (22), integrating by parts and setting the coefficient δu_0 and δv_0 to zero lead to the following equilibrium equations

$$(EI + l^2\mu A)\left(\frac{\partial^4 v_0}{\partial X^4}\right) - q = 0 \tag{23}$$

2.3 Crack modeling

The cracked beam is modelled using a proper modification of the classical cracked-beam theory consisting of two sub-beams connected through a massless elastic rotational spring shown in Fig. 2. The crack is assumed as perpendicular to beam surface and always remains open. The crack is located at a distance L_1 from the left end.

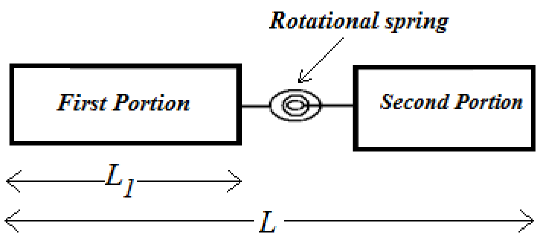

Fig. 2 Rotational spring model

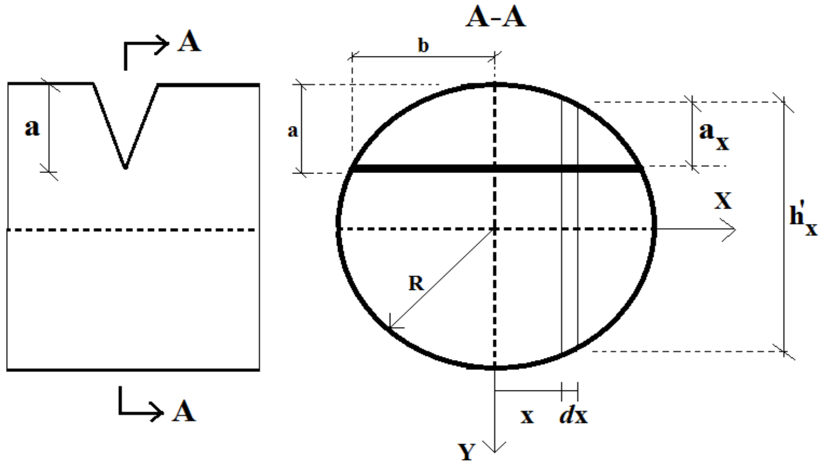

Fig. 3 The geometry of the cracked circular cross section

In the crack section, the additional strain energy is obtained by using linear fracture mechanics. With using the energy release rate approach, cracked section's flexibility G can be derived from Broek's approximation (Broek 1986)

$$\frac{(1-\nu^2)\mathrm{K}_I^2}{E} = \frac{M^2}{2}\frac{\mathrm{dG}}{\mathrm{da}} \tag{24}$$

where M is the bending moment at the cracked section, a is crack of depth, K_I is the stress intensity factor (SIF) under mode I bending load and is a function of the geometry and the loading properties as well. ν indicates Poisson's ratio. For circular cross section, the stress intensity factor for K_I a single edge cracked beam specimen under pure bending M can be written as follow (Tada *et al*. 1985)

$$K_I = \frac{4M}{\pi R^4}\frac{h_X^{'}}{2}\sqrt{\pi a}\, F\left(a/h_X^{'}\right) \tag{25}$$

where

$$F\left(a/h_X^{'}\right) = \sqrt{\frac{2h_X^{'}}{\pi a} tg\left(\frac{\pi a}{2h_X^{'}}\right)}\; \frac{0.923+0.199\left(1-sin\left(\frac{\pi a}{2h_X^{'}}\right)\right)^4}{cos\left(\frac{\pi a}{2h_X^{'}}\right)} \tag{26}$$

where a is crack of depth and $h_X^{'}$ is the height of the strip, is shown Fig. 3, and written as

$$h_X^{'} = 2\sqrt{R^2 - x^2} \tag{27}$$

where R is the radius of the cross section of the beam.

After substituting Eq. (25) into Eq. (24) and by integrating Eq. (24), the flexibility coefficient of the crack section G is obtained as

$$G = \frac{32(1-\nu^2)}{E\pi R^8}\int_{-b}^{b}\int_{0}^{a_x} y(R^2 - x^2)\, F^2\left(a/h_X^{'}\right)\, dy\, dx \tag{28}$$

where b and a_x are the boundary of the strip and the local crack depth respectively, are shown in

Fig. 3, respectively, and written as

$$b = \sqrt{R^2 - (R-a)^2} \tag{29}$$

$$\mathrm{a}_x = \sqrt{R^2 - x^2} - (R-a) \tag{30}$$

The bending stiffness of the cracked section k_T is related to the flexibility G by

$$k_T = \frac{1}{G} \tag{31}$$

2.4 Analytical solution of cracked microbeams

It is mentioned before that, there are two different portions in the beam because of the crack. Hence, there are two different expressions for static deflection equation of the cracked beam. Eq. (23) for deflection curve is written for each portion as follows

$$(EI + l^2\mu A)\, v_1''''(x) - q = 0, \qquad 0 \ll \mathrm{x} \ll \mathrm{L}_1 \tag{32a}$$

$$(EI + l^2\mu A)\, v_2''''(x) - q = 0, \qquad \mathrm{L}_1 \ll \mathrm{x} \ll \mathrm{L} \tag{32b}$$

where $v_1(x)$ is the function which defines the elastic curve for first portion (Between the left support and the crack) and $v_2(x)$ is the function which defines the elastic curve for second portion (Between the crack and the right support). The above two equations have eight unknown constants that must get satisfied by four boundary condition at two beam ends and four following compatibility conditions at the cracked section. The spring connects the adjacent left and right elements and couples the slopes of the two beam elements at the crack location. In the massless spring model, the compatibility conditions enforce the continuities of the transverse deflection, shear force bending moment and shear force across the crack at the cracked section (x=L_1),

Continuity of the vertical displacement

$$v_1(L_1) = v_2(L_1) \tag{33}$$

Continuity of the bending moment

$$(EI + l^2\mu A)\, v_1''(L_1) = (EI + l^2\mu A)\, v_2''(L_1) \tag{34}$$

Continuity of the shear force

$$(EI + l^2\mu A)\, v_1'''(L_1) = (EI + l^2\mu A)\, v_2'''(L_1) \tag{35}$$

Discontinuity of the slope

$$\mathrm{k_T}(v_1'(L_1) - v_2'(L_1)) = k_T(\Delta\theta) = M_1 \tag{36}$$

where M_1 is the bending moment at the cracked section.

By integrating Eqs. (32a) and (32b) four times, the following equations are obtained with unknown coefficients

For first portion (between the left support and the crack)

$$(EI + l^2\mu A)\, v_1''''(x) = q, \qquad 0 \ll \mathrm{x} \ll L_1 \tag{37a}$$

$$(EI + l^2\mu A)\, v_1''' = qx + C_1 \tag{37b}$$

$$(EI + l^2\mu A)\, v_1'' = \frac{1}{2}qx^2 + C_1 x + C_2 \tag{37c}$$

$$(EI + l^2\mu A)\, v_1' = \frac{1}{6}qx^3 + \frac{1}{2}C_1x^2 + C_2x + C_3 \tag{37d}$$

$$(EI + l^2\mu A)\, v_1 = \frac{1}{24}qx^4 + \frac{1}{6}C_1x^3 + \frac{1}{2}C_2x^2 + C_3x + C_4 \tag{37e}$$

For second portion (between the crack and the right support)

$$(EI + l^2\mu A)\, v_2''''(x) = q, \qquad L_1 \ll \mathrm{x} \ll L \tag{38a}$$

$$(EI + l^2\mu A)\, v_2''' = qx + D_1 \tag{38b}$$

$$(EI + l^2\mu A)\, v_2'' = \frac{1}{2}qx^2 + D_1x + D_2 \tag{38c}$$

$$(EI + l^2\mu A)\, v_2' = \frac{1}{6}qx^3 + \frac{1}{2}D_1x^2 + D_2x + D_3 \tag{38d}$$

$$(EI + l^2\mu A)\, v_2 = \frac{1}{24}qx^4 + \frac{1}{6}D_1x^3 + \frac{1}{2}D_2x^2 + D_3x + D_4 \tag{38e}$$

where C_1, C_2, C_3, C_4, D_1, D_2, D_3 and D_4 are the constants of integration which is to adjusted to satisfy the conditions. In this paper, the elastic curve functions of the micro beams are obtained in explicit form for cantilever and simply supported beams.

2.4.1 Cantilever beam

For cantilever beam, the boundary conditions and evaluated constants of integration are expressed as

$$v_1(0) = 0 \tag{39a}$$

$$v_1'(0) = 0 \tag{39b}$$

$$v_2''(\mathrm{L}) = 0 \tag{39c}$$

$$v_2'''(\mathrm{L}) = 0 \tag{39d}$$

$$\mathrm{C}_4 = 0 \tag{39e}$$

$$\mathrm{C}_3 = 0 \tag{39f}$$

$$\mathrm{D}_1 = -qL \tag{39g}$$

$$\mathrm{D}_2 = qL^2/2 \tag{39h}$$

The other constants of integration are determined by using the boundary conditions of the crack section (x=L_1) which is given Eqs. (33)-(36)

$$\mathrm{C}_1 = -qL \tag{40a}$$

$$\mathrm{C}_2 = qL^2/2 \tag{40b}$$

$$\mathrm{D}_3 = -\frac{1}{2}\frac{(EI+l^2\mu A)}{k_T}q(L - L_1)^2 \tag{40c}$$

$$\mathrm{D}_4 = \frac{1}{2}\frac{(EI+l^2\mu A)}{k_T}q(L - L_1)^2\, L_1 \tag{40d}$$

After substituting the determined constants of integration into Eq. (37e) and (38e), the elastic curves of the cracked cantilever microbeam are expressed as

$$v_1(x) = \frac{q}{(EI+l^2\mu A)}\left(\frac{x^4}{24} - \frac{L\,x^3}{6} + \frac{L^2x^2}{4}\right) \tag{41a}$$

$$v_2(x) = \frac{q}{(EI+l^2\mu A)}\left(\frac{x^4}{24} - \frac{L\,x^3}{6} + \frac{L^2x^2}{4} + \frac{1}{2}\frac{(EI+l^2\mu A)}{\mathrm{k_T}}(L-L_1)^2(X-L_1)\right) \tag{41b}$$

2.4.2 Simple supported beam

For simple supported beam, the boundary conditions and evaluated constants of integration are expressed as

$$v_1(0) = 0 \tag{42a}$$

$$v_1''(0) = 0 \tag{42b}$$

$$v_2(\mathrm{L}) = 0 \tag{42c}$$

$$v_2''(\mathrm{L}) = 0 \tag{42d}$$

$$\mathrm{C}_4 = 0 \tag{42e}$$

$$\mathrm{C}_2 = 0 \tag{39f}$$

The other constants of integration are determined by using the boundary conditions of the crack section (x=L_1) which is given Eqs. (33)-(36)

$$\mathrm{C}_1 = -qL/2 \tag{43a}$$

$$\mathrm{C}_3 = \frac{qL^3}{24} + \frac{1}{2}\frac{(EI+l^2\mu A)}{k_T}q(L-L_1)^2\frac{L_1}{L} \tag{43b}$$

$$\mathrm{D}_1 = -qL/2 \tag{43c}$$

$$\mathrm{D}_2 = 0 \tag{43d}$$

$$\mathrm{D}_3 = \frac{qL^3}{24} - \frac{1}{2}\frac{(EI+l^2\mu A)}{k_T}q(L-L_1)\frac{{L_1}^2}{L} \tag{43e}$$

$$\mathrm{D}_4 = \frac{1}{2}\frac{(EI+l^2\mu A)}{k_T}q(L-L_1){L_1}^2 \tag{43f}$$

After substituting the determined constants of integration into Eqs. (37e) and (38e), the elastic curves of the cracked simple supported microbeam are expressed as

$$v_1(x) = \frac{q}{(EI+l^2\mu A)}\left(\frac{x^4}{24} - \frac{L\,x^3}{12} + \left(\frac{L^3}{24} + \frac{1}{2}\frac{(EI+l^2\mu A)}{k_T}(L-L_1)^2\frac{L_1}{L}\right)x\right) \tag{44a}$$

$$v_2(x) = \frac{q}{(EI+l^2\mu A)}\left(\frac{x^4}{24} - \frac{L\,x^3}{12} + \left(\frac{L^3}{24} - \frac{1}{2}\frac{(EI+l^2\mu A)}{k_T}(L-L_1)\frac{{L_1}^2}{L}\right)x + \frac{1}{2}\frac{(EI+l^2\mu A)}{k_T}(L-L_1){L_1}^2\right) \tag{44b}$$

The dimensionless quantities can be expressed as

$$\overline{\mathrm{X}} = \frac{X}{L}, \overline{\mathrm{Y}} = \frac{Y}{L}, \bar{\mathrm{v}} = \frac{v}{L}, \eta = \frac{L_1}{L}, a_r = \frac{a}{D} \tag{45}$$

where, η is the ratio of crack location and a_r is the ratio of crack depth.

3. Numerical results

In the numerical examples, the effects of the location of crack (η), the depth of the crack (a_r), aspect ratio (L/D) and the dimensionless material length scale parameter (D/l) on the static

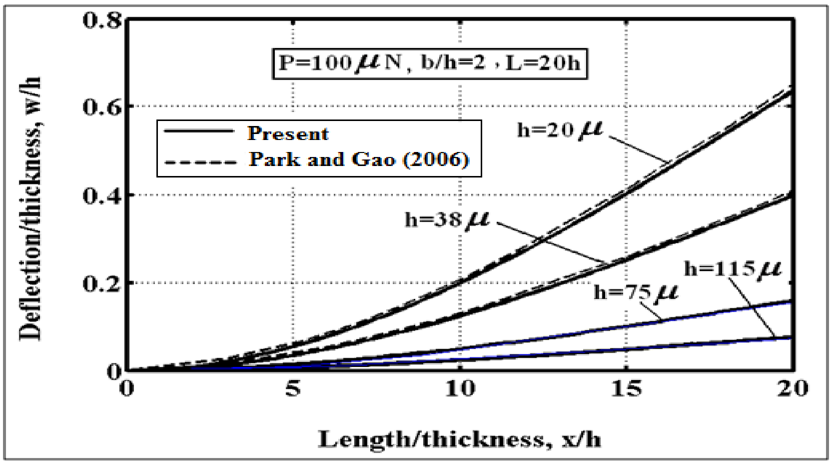

Fig. 4 Deflections of the cantilever beam based on the MCST

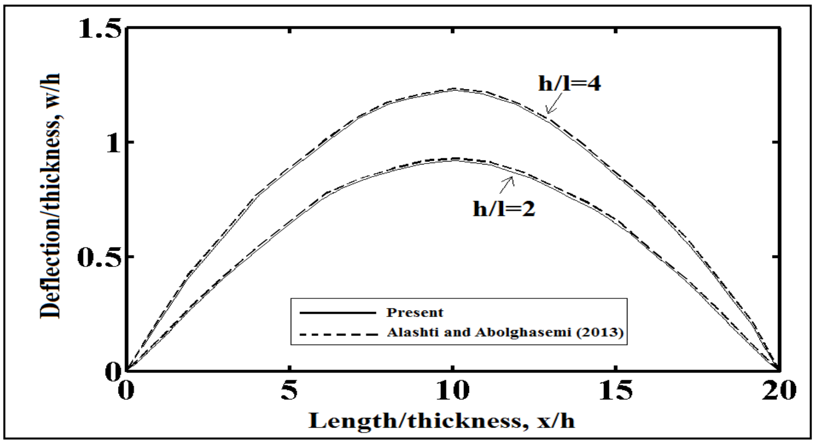

Fig. 5 Deflections of the simple supported beam based on the MCST

deflection of the micro beams are presented in both the MCST and the CBT in tables and figures. The beam is taken to be made of epoxy (E=1,44 GPa, $\nu = 0.38, l = 17.6\,\mu$m). For investigation of the size effect in the micro beam, the dimensionless material length scale parameter (D/l) is described in the MCST.

In order to establish the accuracy of the present formulation and the computer program developed by the author, the results obtained from the present study are compared with the available results in the literature. For this purpose, static deflections of a cantilever intact beam with rectangular cross section which is subjected to a point load are calculated for modified couple stress theory and compared with those of Park and Gao (2006). It is clearly seen that the curves of Fig. 4 of the present study are very close to those of Fig. 3 of Park and Gao (2006).

To further verify the present results, the static deflections shapes of a simple supported intact microbeam with rectangular cross section which is subjected to uniform distributed load are calculated using the MCST and are compared with those of Alashti and Abolghasemi (2013) by inserting the material and load properties used in this reference. A comparison of Fig. 5 with Fig. 6

Table 1 Maximum dimensionless of vertical displacements edge cracked cantilever and simple supported micro beams with different the crack depth ratios (a_r) and the dimensionless material length scale parameter (*D/l*) for distributed load q=10 $\mu N/\mu$m, *L/D*=20 and η=0.5

	Edge Cracked Cantilever Micro Beam							
	MCST				CBT			
D/l	Intact	a_r=0.1	a_r=0.2	a_r=0.3	Intact	a_r=0.1	a_r=0.2	a_r=0.3
2	1.6409	1.6456	1.6653	1.7145	4.0191	4.0237	4.0435	4.0927
3	1.6297	1.6328	1.6459	1.6787	2.6794	2.6825	2.6956	2.7799
5	1.3050	1.3069	1.3148	1.3345	1.6076	1.6095	1.6174	1.6371
8	0.9213	0.9225	0.9274	0.9397	1.0048	1.0059	1.0109	1.0232
10	0.7598	0.7607	0.7646	0.7745	0.8038	0.8047	0.8087	0.8185
15	0.5224	0.5230	0.5257	0.5322	0.5359	0.5365	0.5391	0.5457
20	0.3962	0.3966	0.3962	0.4035	0.4019	0.4024	0.4043	0.4093
30	0.2662	0.2665	0.2678	0.2711	0.2679	0.2682	0.2696	0.2728
50	0.1604	0.1606	0.1614	0.1633	0.1608	0.1609	0.1617	0.1637
	Edge Cracked Simple Supported Micro Beam							
	MCST				CBT			
D/l	Intact	a_r=*0.1*	a_r=*0.2*	a_r=*0.3*	Intact	a_r=*0.1*	a_r=*0.2*	a_r=*0.3*
2	0.1709	0.1733	0.1831	0.2077	0.4187	0.4210	0.4308	0.4555
3	0.1698	0.1713	0.1779	0.1943	0.2791	0.2806	0.2872	0.3036
5	0.1359	0.1369	0.1408	0.1507	0.1675	0.1684	0.1723	0.1822
8	0.0960	0.0966	0.0990	0.1052	0.1047	0.1052	0.1077	0.1139
10	0.0791	0.0796	0.0816	0.0865	0.0837	0.0842	0.0862	0.0911
15	0.0544	0.0547	0.0560	0.0593	0.0558	0.0561	0.0574	0.0607
20	0.0413	0.0415	0.0425	0.0449	0.0419	0.0421	0.0431	0.0455
30	0.0277	0.0279	0.0285	0.0302	0.0279	0.0281	0.0287	0.0304
50	0.0167	0.0168	0.0172	0.0182	0.0167	0.0168	0.0172	0.0182

of Alashti and Abolghasemi (2013) shows that the present results are close to those of Alashti and Abolghasemi (2013).

In order to investigate the size effect and the crack depth ratios (a_r), the maximum dimensionless vertical displacements of edge cracked cantilever and simple supported micro beams are presented with different the crack depth ratios (a_r) and the dimensionless material length scale parameter (*D/l*) for MCST and CBT for distributed load q=10 μN/μm, *L/D*=20 and η=0.5 in Table 1.

As seen from Table 1, with the increase in the crack depth, the displacements increase, as expected. This is because by increasing the crack depth ratio, the beam becomes flexible. It can be noticed that the results predicted by the MCST are always smaller than those of the CBT. Further, the difference between the two results is remarkable for thin microbeams with *D/l* <10. Also, it is seen from Table 1 that with the decrease in the crack depth, the difference between the results of the MCST and CBT decrease considerably. It shows that an increase in the *D/l* ratio leads to a decline on effects of size effect and difference between the results of MCST and CBT diminishes

Table 2 Maximum dimensionless vertical displacements of edge cracked cantilever and simple supported micro beams with different the crack locations (η) and the dimensionless material length scale parameter (*D/l*) for distributed load q=10μN/ μm, *L/D*=20 and a_r=0.3

	Edge Cracked Cantilever Micro Beam							
	MCST				CBT			
D/l	Intact	η=0.5	η=0.3	η=0.1	Intact	η=0.5	η=0.3	η=0.1
2	1.6409	1.7145	1.8429	2.0702	4.0191	4.0927	4.0191	4.4483
3	1.6297	1.6787	1.7643	1.9159	2.6794	2.7284	2.8140	2.9656
5	1.3050	1.3345	1.3858	1.4767	1.6076	1.6371	1.6884	1.7793
8	0.9213	0.9397	0.9718	1.0286	1.0048	1.0232	1.0553	1.1121
10	0.7598	0.7745	0.8002	0.8456	0.8038	0.8185	0.8442	0.8897
15	0.5224	0.5322	0.5493	0.5797	0.5359	0.5457	0.5628	0.5931
20	0.3962	0.4035	0.4164	0.4391	0.4019	0.4093	0.4221	0.4448
30	0.2662	0.2711	0.2797	0.2948	0.2679	0.2728	0.2814	0.2966
50	0.1604	0.1633	0.1685	0.1776	0.1608	0.1637	0.1688	0.1779
	Edge Cracked Simple Supported Micro Beam							
	MCST				CBT			
D/l	Intact	η=0.5	η=0.3	η=0.1	Intact	η=0.5	η=0.3	η=0.1
2	0.1709	0.2077	0.1899	0.1736	0.4187	0.4555	0.4374	0.4213
3	0.1698	0.1943	0.1823	0.1715	0.2791	0.3036	0.2916	0.2809
5	0.1359	0.1507	0.1434	0.1370	0.1675	0.1822	0.1749	0.1685
8	0.0960	0.1052	0.1007	0.0966	0.1047	0.1139	0.1093	0.1053
10	0.0791	0.0865	0.0829	0.0797	0.0837	0.0911	0.0875	0.0843
15	0.0544	0.0593	0.0569	0.0548	0.0558	0.0607	0.0583	0.0562
20	0.0413	0.0449	0.0431	0.0415	0.0419	0.0455	0.0437	0.0421
30	0.0277	0.0302	0.0290	0.0279	0.0279	0.0304	0.0292	0.0281
50	0.0167	0.0182	0.0175	0.0168	0.0167	0.0182	0.0175	0.0169

for *D/l* > 30.

In Table 2, the maximum dimensionless vertical displacements of edge cracked cantilever and simple supported micro beams are presented with different the crack locations (η) and the dimensionless material length scale parameter (*D/l*) for MCST and CBT for distributed load q=10μN/μm, *L/d*=20 and a_r=0.3.

It is seen from Table 2 that when the crack locations get closer to the left end of the beam, the displacements increase for cantilever beam. This is because the crack at the left end of the beam has a most severe effect in the cantilever beam. Whereas, the crack locations get closer to the midpoint of the beam, the displacements increase for simple supported beam because the crack at the midpoint of the beam has a most severe effect for simple supported beam. As stated before, the material parameter has a very important role on the static behavior of the edge cracked micro beams, and it should be considered in the static and dynamic analysis of micro beams. Also, it is believed that the tabulated results will be a reference with which other researchers can compare their results.

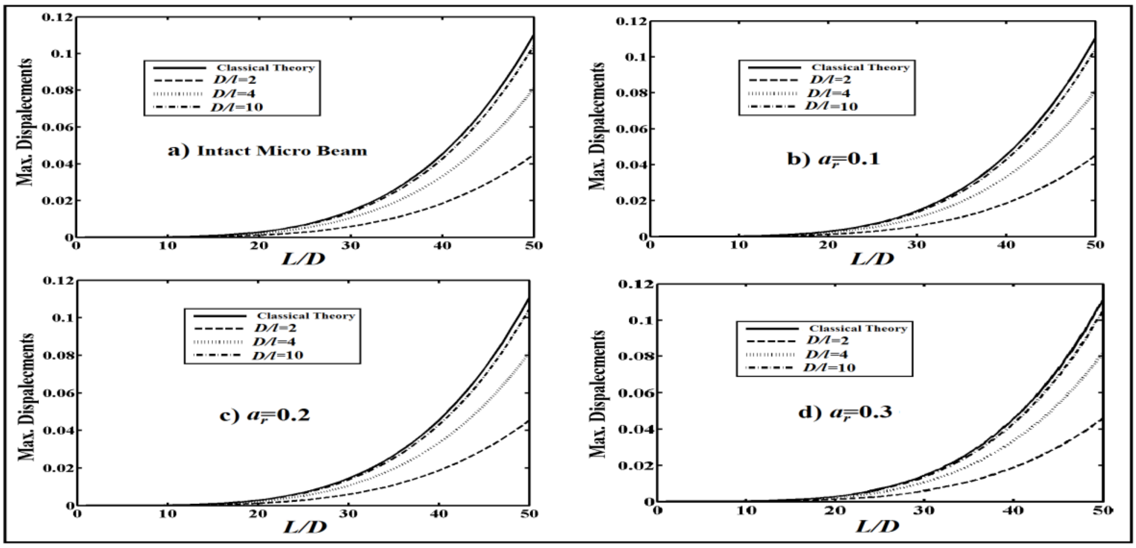

Fig. 6 Maximum vertical displacements of edge cracked cantilever micro beam with different the a_r and the *L/D*) for q=10μN/μm and η=0.5

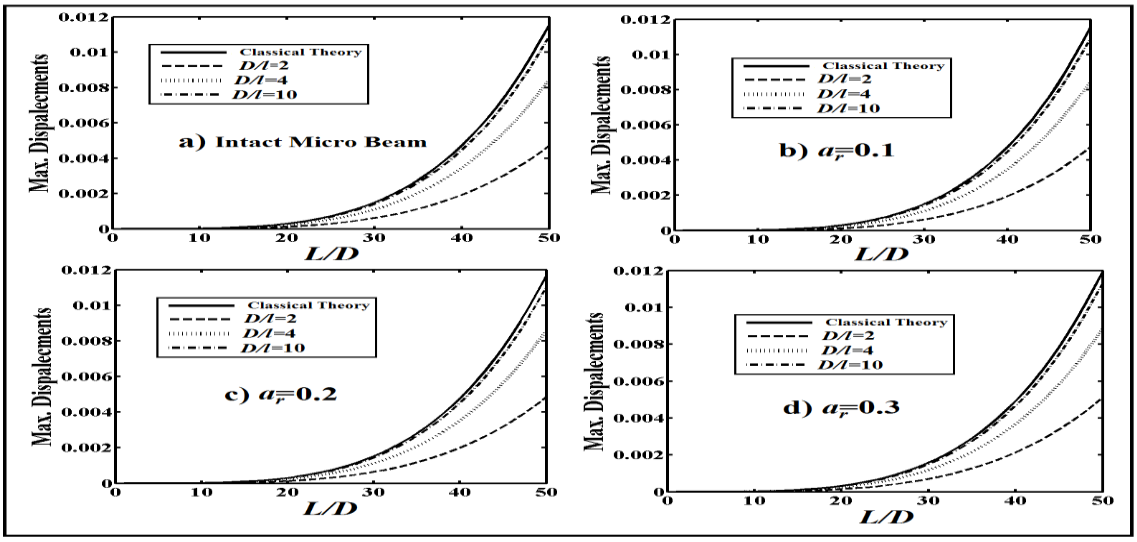

Fig. 7 Maximum vertical displacements of edge cracked simple supported micro beam with different the a_r and the *L/D* for q=10μN/μm and η=0.5

Also it is seen from Table 2 that with change the crack locations, the results of the MCST are more sensitive than the results of the CBT. This is because the using the classical cracked-beam theory. On the other hand, increase in the *D/l* ratio, the difference between results of the MCST and CBT decrease considerably for different ratio of the crack locations (η). It is observed from tables that for the higher ratio of *D/l*, the classical cracked-beam theory can be used for the cracked problems of the microbeams.

In Figs. 6 and 7, the effect of the aspect ratios (*L/D*) and the crack depth ratios (a_r) on the

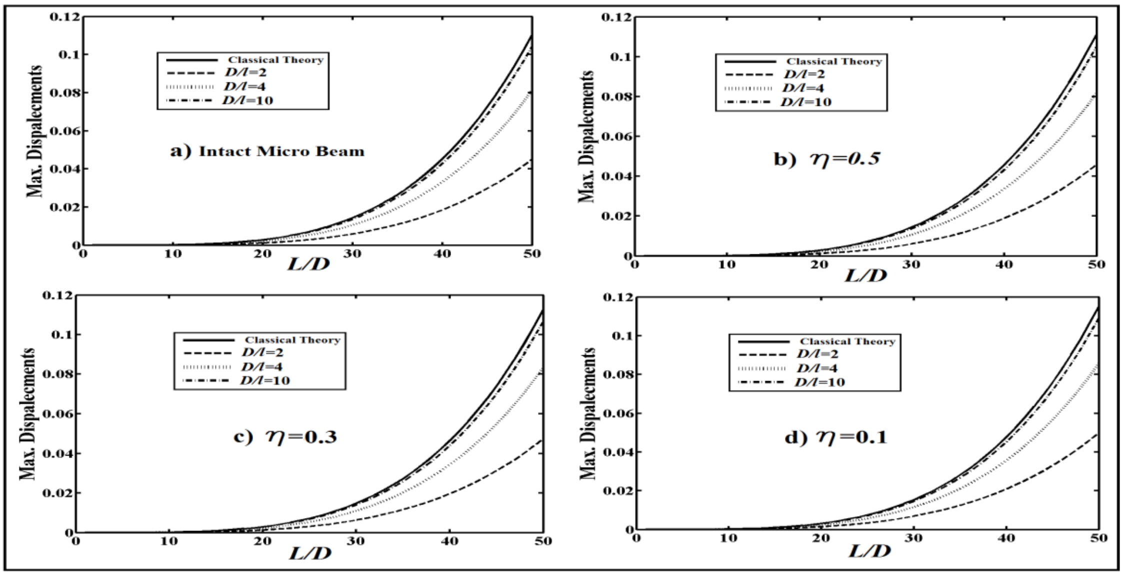

Fig. 8 Maximum vertical displacements of edge cracked cantilever micro beam with different the η and the *L/D*) for q=10$\mu N/\mu m$ and a_r=0.3

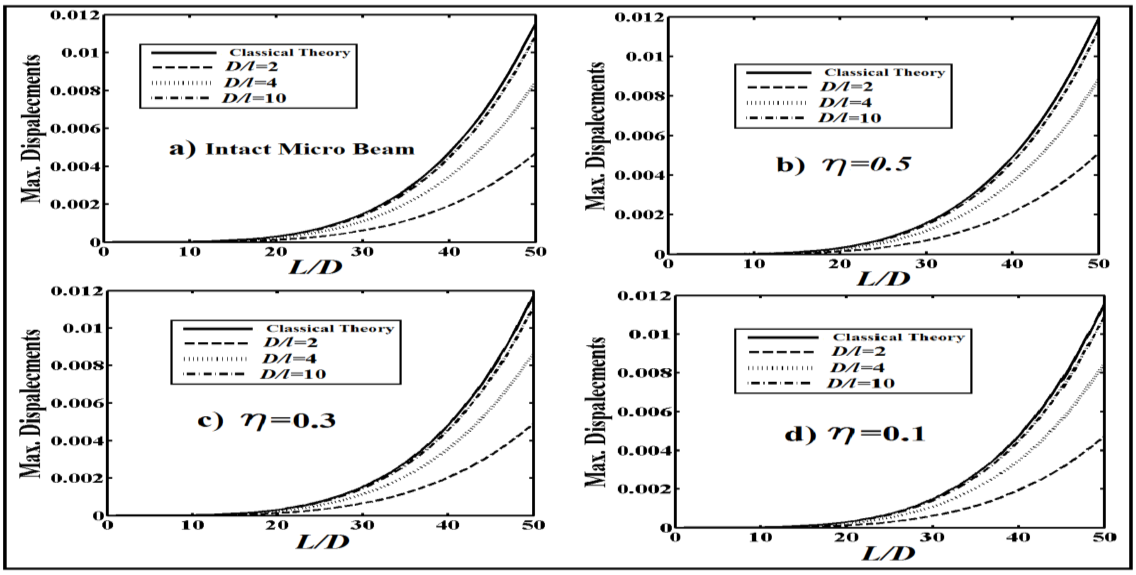

Fig. 9 Maximum vertical displacements of edge cracked simple supported micro beam with different the η and the *L/D* for q=10μN/μm and a_r=0.3

maximum the vertical displacements of the micro beams are shown for q=10μN/ μm and η=0.5 for cantilever and simple supported beams, respectively. Also, the relationship between the *L/D* and *D/l* is investigated in Figs. 6 and 7.

In Figs. 8 and 9, the effect of the aspect ratio and the crack location ratios (η) on the maximum the vertical displacements of the micro beams are shown for q=10μN/ μm and a_r=0.3 for cantilever and simple supported beams, respectively.

As seen from Figs. 6, 7, 8 and 9, the material length scale parameter has no effect on the displacements for the classical beam theory, which is unable to capture the size effect. However, the displacements of the non classical beam model increases as the material length scale parameter increases. The static deflections estimated by the CBT is always larger than those of the MCST. It is observed from figures that the difference between the two models is significant when the ratio of *L/D* increases for the smaller ratio of *D/l*. Whereas, with increase in the ratio of *L/D*, the difference between the static deflections of the MCST and CBT decrease considerably for the higher ratio of *D/l*. Also, it is seen from Figs. 6, 7, 8 and 9 that with increase in values of the crack depth and locations, the deflections increase in small amounts with all values of the ratio of *L/D*.

Figs. 10 and 11 display the crack depth ratios (a_r) on the deflected shape of the beams for the crack location ratio η=0.5 and for q=10μN/ μm for different ratios of *L/D* and *D/l* for cantilever and simple supported micro beams, respectively.

It is observed from Figs. 10 and 11 that with increase in the ratio of *D/l*, the effects of the cracks on the static responses of the micro beams are decrease significantly. With increase in the ratio of *D/l*, the difference among the crack depth ratios diminishes. It shows that the material parameter has a very important role on the effects of the cracks on the static responses of the micro beams. Also, it is seen from Figs. 10 and 11 that when the ratio of *L/D* increases, the effects of the

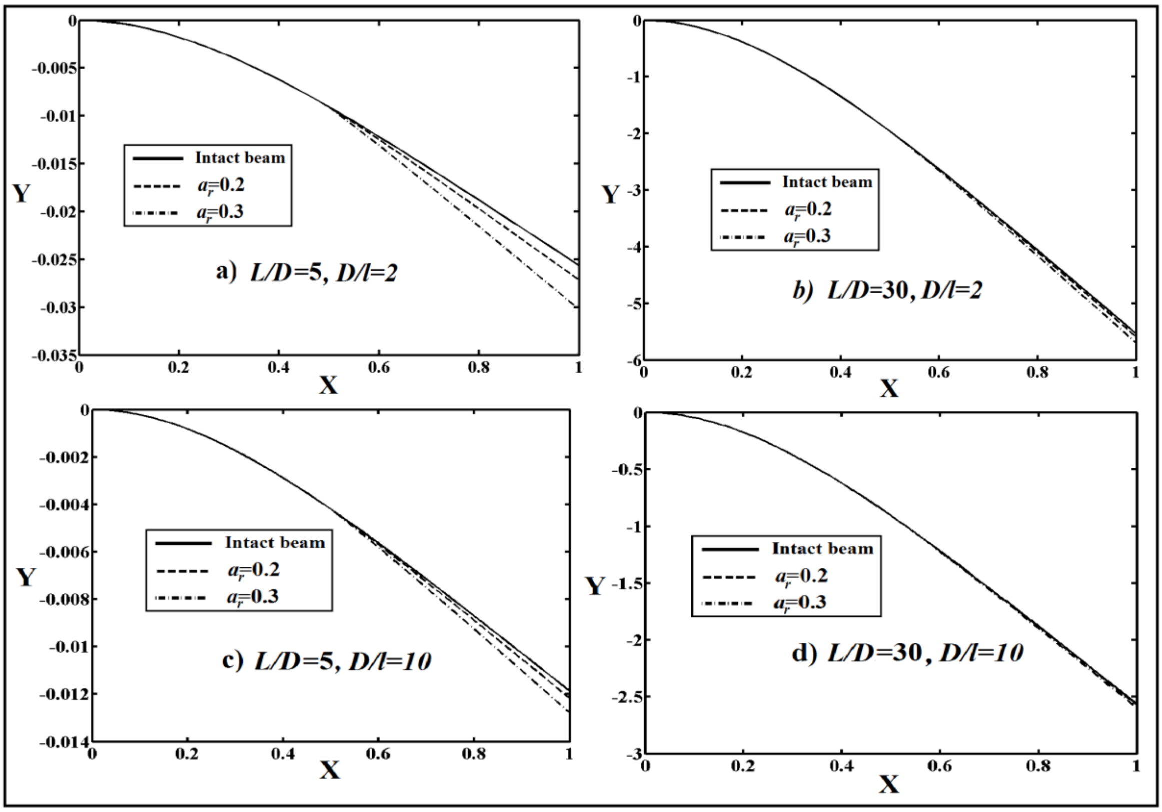

Fig. 10 The effect of the a_r on the deflected shape of the cantilever micro beam for (a) *L/D*=5, *D/l*=2, (b) *L/D*=30, *D/l*=2, (c) *L/D*=5, *D/l*=10, (d) *L/D*=30, *D/l*=10

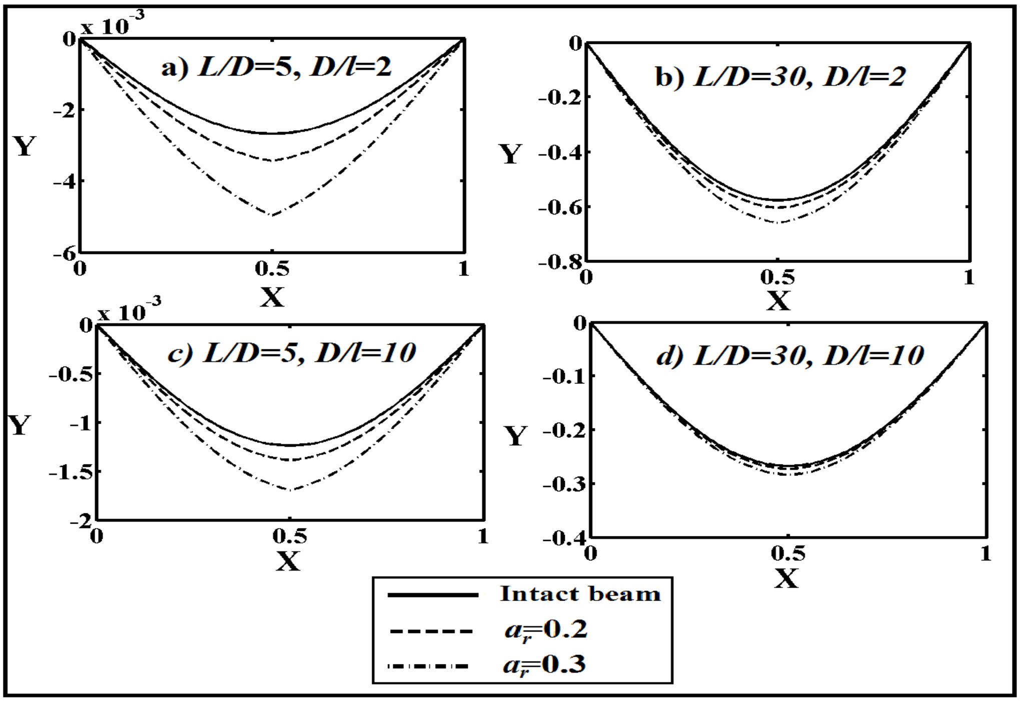

Fig. 11 The effect of the a_r on the deflected shape of the simple supported micro beam for (a) *L/D*=5, *D/l*=2, (b) *L/D*=30, *D/l*=2, (c) *L/D*=5, *D/l*=10, (d) *L/D*=30, *D/l*=10

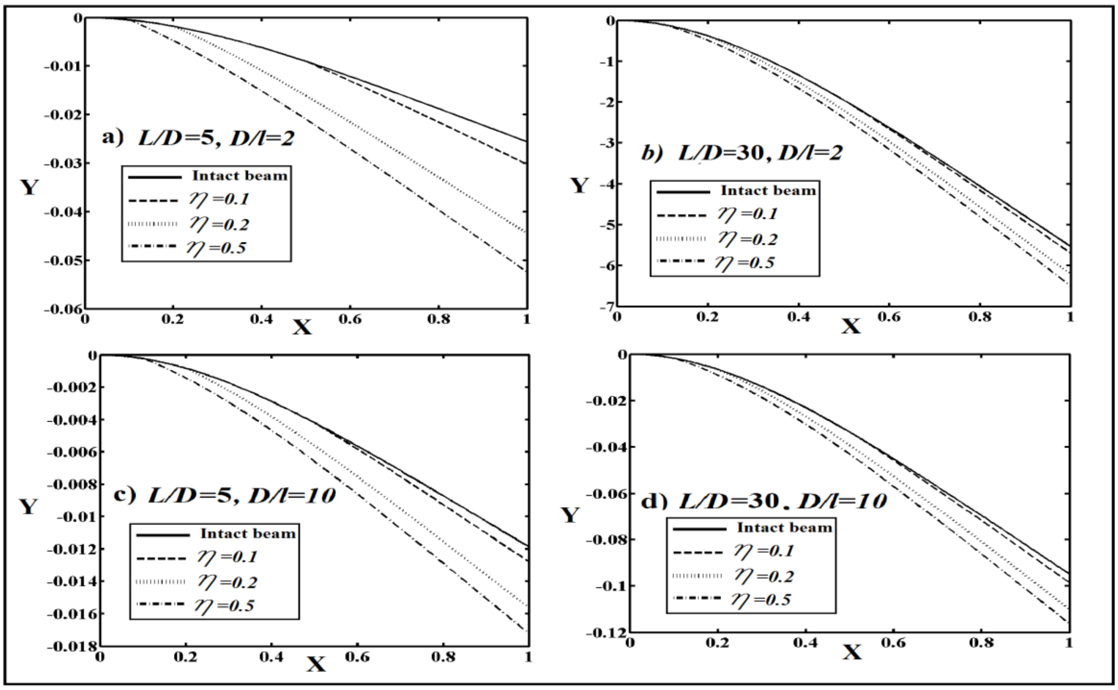

Fig. 12 The effect of the η on the deflected shape of the cantilever micro beam for (a) *L/D*=5, *D/l*=2, (b) *L/D*=30, *D/l*=2, (c) *L/D*=5, *D/l*=10, (d) *L/D*=30, *D/l*=10

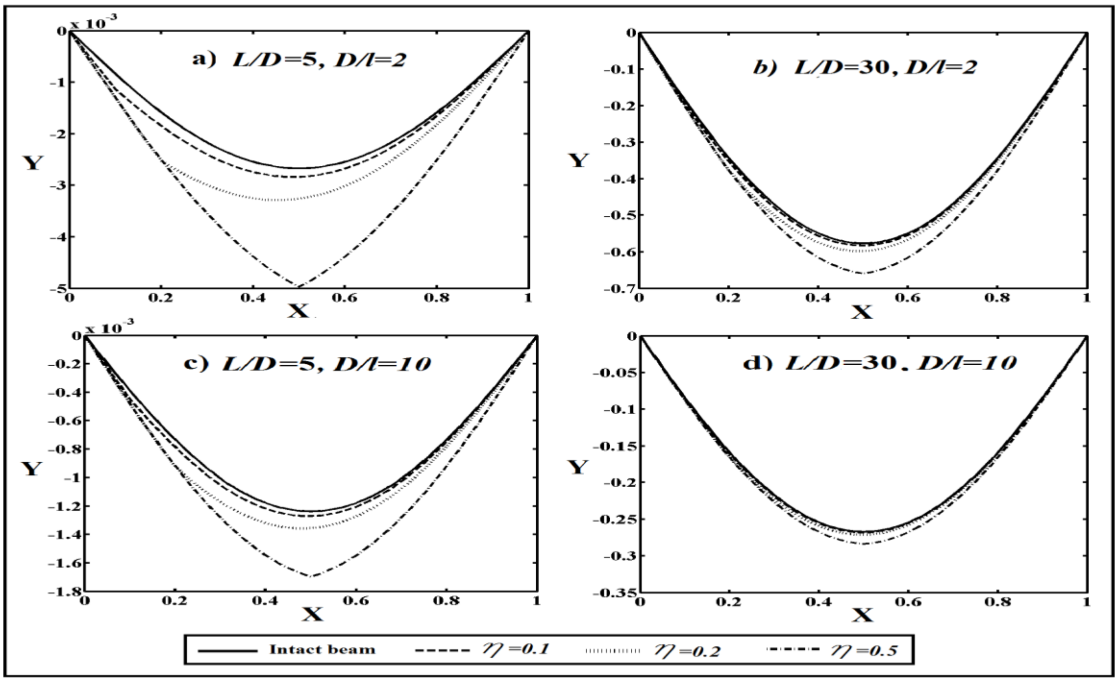

Fig. 13 The effect of the η on the deflected shape of the simple supported micro beam for (a) *L/D*=5, *D/l*=2, (b) *L/D*=30, *D/l*=2, (c) *L/D*=5, *D/l*=10, (d) *L/D*=30, *D/l*=10

crack depth ratios on the static responses of the micro beams are decrease significantly.

In Fig. 12 and 13, the crack location ratios (η) on the deflected shape of the micro beams for the crack depth ratio $a_r = 0.3$ and for q=10μN/ μm for different ratios of *L/D* and *D/l* for cantilever and simple supported beams, respectively.

As seen from Figs. 12 and 13 that with increase in the ratio of *D/l* and *L/D*, the difference among the crack location ratios decreases. It is clearly seen from Figs. 10-13 that, the geometry properties of the micro beam play an important role in on the effects of the cracks on the static responses of the micro beams and distinguish the difference between the results of MCST and CBT. It is observed from figures that after a certain value of the ratio of *D/l* and *L/D*, the classical cracked-beam model can be used for the cracked problems of the micro beams.

4. Conclusions

This paper examines the static bending of edge cracked micro beams analytically based on MCST. The micro beam is modelled in consist of the material length scale parameter which take into account the size effect. The cracked micro beam was modelled using a rotational spring which promotes a discontinuity in the slope. The elastic curve functions of the edge cracked micro beams are obtained in explicit form for cantilever and simply supported beams. The elastic deflections of the edge cracked micro beams are calculated and discussed for different crack positions, different lengths of the micro beam, different length scale parameter, different crack depths, and some typical boundary conditions. In order to establish the accuracy of the present formulation and results, the deflections are obtained, and compared with the published results available in the literature. Good agreement is observed.

The following conclusions are reached from the obtained results:

(1) It is found that the deflections of the microbeam by the CBT are always larger than those by the MCST.

(2) The geometry properties and the material length scale parameter have a very important role on the static behavior of the edge cracked microbeams.

(3) With increase in the material length scale parameter leads to a decline on effect of size effect, the crack, and difference between the results of MCST and CBT.

(4) The classical cracked-beam theory can be used for the cracked problems of the microbeams for the higher ratio of *D/l*.

(5) With increase in values of the crack depth and locations, the deflections increase in small amounts with all values of the ratio of *L/D*.

(6) For the smaller ratio of *L*/*D*, the MCST must be used instead of the CBT.

(7) MCST displays important size-dependence in small values of the *L/D* and *D/*l ratios.

(8) It is believed that the tabulated results will be a reference with which other researchers can compare their results.

References

Akbaş, Ş.D. (2016), "Free vibration of edge cracked functionally graded microscale beams based on the modified couple stress theory", *Int. J. Struct. Stab. Dyn.*, 1750033.

Akgöz, B. and Civalek, Ö. (2012), "Analysis of microtubules based on strain gradient elasticity and modified couple stress theories", *Adv. Vib. Eng.*, **11**(4), 385-400.

Akgöz, B. and Civalek, Ö. (2013), "Buckling analysis of linearly tapered micro-columns based on strain gradient elasticity", *Struct. Eng. Mech.*, **48**(2), 195-205.

Alashti, R.A. and Abolghasemi, A.H. (2013), "A size-dependent Bernoulli-Euler beam formulation based on a new model of couple stress theory", *Int. J. Eng. Tran. C: Aspect.*, **27**(6), 951.

Ansari, R., Ashrafi, M.A. and Arjangpay, A. (2015), "An exact solution for vibrations of postbuckled microscale beams based on the modified couple stress theory", *Appl. Math. Model.*, **39**(10-11), 3050-3062.

Ansari, R., Gholami, R. and Darabi, M.A. (2012), "A nonlinear Timoshenko beam formulation based on strain gradient theory", *J. Mech. Mater. Struct.*, **7**(2), 95-211.

Asghari, M., Ahmadian, M.T., Kahrobaiyan, M.H. and Rahaeifard, M. (2010), "On the size dependent behavior of functionally graded micro-beams", *Mater. Des.*, **31**, 2324-3249.

Ataei, H., Beni, Y.T. and Shojaeian, M. (2016), "The effect of small scale and intermolecular forces on the pull-in instability and free vibration of functionally graded nano-switches", *J. Mech. Sci. Tech.*, **30**(4), 1799-1816.

Beni, Y.T. and Zeverdejani, M.K. (2015), "Free vibration of microtubules as elastic shell model based on modified couple stress theory", *J. Mech. Med. Biol.*, **15**(03), 1550037.

Beni, Y.T., Jafari, A. and Razavi, H. (2015), "Size effect on free transverse vibration of cracked nano-beams using couple stress theory", *Int. J. Eng.*, **28**(2), 296-304.

Beni, Y.T., Mehralian, F. and Zeighampour, H. (2016), "The modified couple stress functionally graded cylindrical thin shell formulation", *Mech. Adv. Mater. Struct.*, **23**(7), 791-801.

Broek, D. (1986), *Elementary engineering fracture mechanics*, Martinus Nijhoff Publishers, Dordrecht.

Dai, H.L., Wang, Y.K. and Wang, L. (2015), "Nonlinear dynamics of cantilevered microbeams based on modified couple stress theory", *Int. J. Eng. Sci.*, **94**, 103-112.

Daneshmehr, A.R., Abadi, M.M. and Rajabpoor, A. (2013), “Thermal effect on static bending, vibration and buckling of reddy beam based on modified couple stress theory”, *Appl. Mech. Mater.,* **332**,331-338.

Darijani, H. and Mohammadabadi, H. (2014), “A new deformation beam theory for static and dynamic analysis of microbeams”, *Int. J. Mech. Sci.*, **89**, 31-39.

Eringen, A.C. (1972), “Nonlocal polar elastic continua”, *Int. J. Eng. Sci*., **10**(1), 1-16.

Fang, T.H. and Chang, W.J. (2003b), “Sensitivity analysis of scanning near-field optical microscope probe”, *Opt. Laser Tech.*, **35**(4), 267-271.

Fang, T.H., Chang, W.J. and Liao, S.C. (2003a), “Simulated nanojet ejection process by spreading droplets on a solid surface”, *J. Phys. Condens. Matter.*, **15**(49), 8263-8271.

Farokhi, H. and Ghayesh, M.H. (2015), “Thermo-mechanical dynamics of perfect and imperfect Timoshenko microbeams”, *Int. J. Eng. Sci.*, **91**, 12-33.

Fleck, H.A. and Hutchinson, J.W. (1993), “A phenomenological theory for strain gradient effects in plasticity”, *J. Mech. Phys. Solid*., **41**, 1825-57.

Ghayesh, M.H., Amabili, M. and Farokhi, H. (2013), “Three-dimensional nonlinear size-dependent behaviour of Timoshenko microbeams”, *Int. J. Eng. Sci.*, **71**, 1-14.

Hasheminejad, B.S.M., Gheshlaghi, B., Mirzaei, Y. and Abbasion, S. (2011), “Free transverse vibrations of cracked nanobeams with surface effects”, *Thin Solid. Film.*, **519**(8), 2477-2482.

Kahrobaiyan, M.H., Asghari, M., Rahaeifard, M. and Ahmadian, M.T. (2010), “Investigation of the size dependent dynamic characteristics of atomic force microscope microcantilevers based on the modified couple stress theory”, *Int. J. Eng. Sci*., **48**, 1985-1994.

Ke, L.L., Wang, Y.S. and Wang, Z.D. (2011), “Thermal effect on free vibration and buckling of size-dependent microbeams”, *Physica E: Low Dimens. Syst. Nanostruct.*, **43**(7), 1387-1393.

Kocatürk, T. and Akbaş, Ş.D. (2013), “Wave propagation in a microbeam based on the modified couple stress theory”, *Struct. Eng. Mech.*, **46**, 417-431.

Kong, S., Zhou, S., Nie, Z. and Wang, K. (2008), “The size-dependent natural frequency of Bernoulli-Euler micro-beams”, *Int. J. Eng. Sci*., **46**, 427-437.

Kong, S.L. (2013), “Size effect on natural frequency of cantilever micro-beams based on a modified couple stress theory”, *Adv. Mater. Res.*, **694-697**, 221-224.

Lam, D.C.C., Yang, F., Chong, A.C.M., Wang, J. and Tong, P. (2003), “Experiments and theory in strain gradient elasticity”, *J. Mech. Phys. Solid.*, **51**(8), 1477-508.

Liu, S.J., Qi, S.H. and Zhang, W.M. (2013), “Vibration behavior of a cracked micro-cantilever beam under electrostatic excitation”, *J. Vib. Shock*, **32**(17), 41-45.

Loya, J., López-Puente, J., Zaera, R. and Fernández-Sáez, J. (2009), “Free transverse vibrations of cracked nanobeams using a nonlocal elasticity model”, *J. Appl. Phys.*, **105**(4), 044309.

Ma, H.M., Gao, X.L. and Reddy, J.N. (2008), “A microstructure-dependent Timoshenko beam model based on a modified couple stress theory”, *J. Mech. Phys. Solid.*, **56**, 3379-3391.

Mindlin, R.D. (1963), “Influence of couple-stresses on stress concentrations”, *Exp. Mech*., **3**, 1-7.

Mindlin, R.D. and Tiersten, H.F. (1962), “Effects of couple-stresses in linear elasticity”, *Arch. Rat. Mech. Anal.*, **11**, 415-48.

Park, S.K. and Gao, X.L. (2006), “Bernoulli-Euler beam model based on a modified couple stress theory”, *J. Micromech. Microeng.*, **16**, 2355-2359.

Pei, J., Tian, F. and Thundat, T. (2004), “Glucose biosensor based on the microcantilever”, *Anal. Chem.*, **76**, 292-297.

Rezazadeh, G., Tahmasebi, A. and Zubtsov, M. (2006), “Application of piezoelectric layers in electrostatic MEM actuators: controlling of pull-in voltage”, *J. Microsyst. Tech.*, **12**, 1163-1170.

Sedighi, H.M. and Bozorgmehri, A. (2016), “Dynamic instability analysis of doubly clamped cylindrical nanowires in the presence of Casimir attraction and surface effects using modified couple stress theory”, *Acta Mechanica*, **227**(6), 575-1591.

Sedighi, H.M., Changizian, M. and Noghrehabadi, A. (2014), “Dynamic pull-in instability of geometrically nonlinear actuated micro-beams based on the modified couple stress theory”, *Lat. Am. J. Solid. Struct.*, **11**(5), 810-825.

Senturia S.D. (1998), "CAD challenges for microsensors, microactuators, and microsystems", *Proc. IEEE*, **86**, 1611-1626.

Shojaeian, M. and Beni, Y.T. (2015), "Size-dependent electromechanical buckling of functionally graded electrostatic nano-bridges", *Sens. Actuat. A: Phys.*, **232**, 49-62.

Shojaeian, M., Beni, Y.T. and Ataei, H. (2016), "Electromechanical buckling of functionally graded electrostatic nanobridges using strain gradient theory", *Acta Astronautica*, **118**, 62-71.

Şimsek, M. (2010), "Dynamic analysis of an embedded microbeam carrying a moving microparticle based on the modified couple stress theory", *Int. J. Eng. Sci*., **48**, 1721-1732.

Şimşek, M., Kocatürk, T. and Akbaş, Ş.D. (2013), "Static bending of a functionally graded microscale Timoshenko beam based on the modified couple stress theory", *Compos. Struct*., **95**, 740-747.

Tada, H., Paris, P.C. and Irwin, G.R. (1985), *The Stress Analysis of Cracks Handbook*, Paris Production Incorporated and Del Research Corporation.

Tang, M., Ni, Q., Wang, L., Luo, Y. and Wang, Y. (2014), "Size-dependent vibration analysis of a microbeam in flow based on modified couple stress theory", *Int. J. Eng. Sci.*, **85**, 20-30.

Torabi, K. and Nafar Dastgerdi, J. (2012), "An analytical method for free vibration analysis of Timoshenko beam theory applied to cracked nanobeams using a nonlocal elasticity model", *Thin Solid. Film*., **520**(21), 6595-6602.

Toupin, R.A. (1962), "Elastic materials with couple stresses", *Arch. Rat. Mech. Anal.*, **11**, 385-414.

Wang, L. (2010), "Size-dependent vibration characteristics of fluid-conveying microtubes", *J. Fluid. Struct.*, **26**, 675-684.

Wang, L., Xu, Y.Y. and Ni, Q. (2013), "Size-dependent vibration analysis of three-dimensional cylindrical microbeams based on modified couple stress theory: a unified treatment", *Int. J. Eng. Sci.*, **68**, 1-10.

Xia, W., Wang, L. and Yin, L. (2010), "Nonlinear non-classical microscale beams: static, bending, postbuckling and free vibration", *Int. J. Eng. Sci.*, **48**, 2044-053.

Yang, F., Chong, A., Lam, D. and Tong, P. (2002) "Couple stress based strain gradient theory for elasticity", *Int. J. Solid. Struct.*, **39**(10), 2731-2743.

Zeighampour, H. and Beni, Y.T. (2014), "Analysis of conical shells in the framework of coupled stresses theory", *Int. J. Eng. Sci.*, **81**, 107-122.

Zeighampour, H. and Beni, Y.T. (2015), "A shear deformable cylindrical shell model based on couple stress theory", *Arch. Appl. Mech.*, **85**(4), 539-553.

Zeighampour, H., Beni, Y.T. and Mehralian, F. (2015), "A shear deformable conical shell formulation in the framework of couple stress theory", *Acta Mechanica*, **226**(8), 2607-2629.

Zook, J.D., Burns, D.W., Guckel, H., Smegowsky, J.J., Englestad, R.L. and Feng, Z. (1992), "Characteristics of polysilicon resonant microbeams", *Sens. Actuat.*, **35**, 31-59.

CC